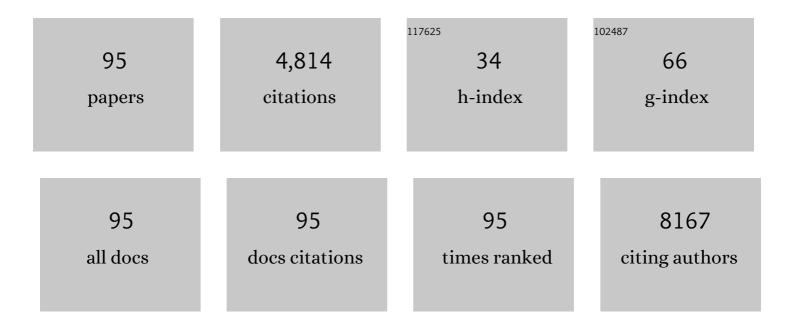
Xiaodong Liu

List of Publications by Year in descending order

Source: https://exaly.com/author-pdf/1160682/publications.pdf Version: 2024-02-01



#	Article	IF	CITATIONS
1	Multigeneration analysis reveals the inheritance, specificity, and patterns of CRISPR/Cas-induced gene modifications in <i>Arabidopsis</i> . Proceedings of the National Academy of Sciences of the United States of America, 2014, 111, 4632-4637.	7.1	669
2	A Selfâ€Assembled Albuminâ€Based Nanoprobe for In Vivo Ratiometric Photoacoustic pH Imaging. Advanced Materials, 2015, 27, 6820-6827.	21.0	244
3	Global pattern for the effect of climate and land cover on water yield. Nature Communications, 2015, 6, 5918.	12.8	236
4	Modulation of auxin content in Arabidopsis confers improved drought stress resistance. Plant Physiology and Biochemistry, 2014, 82, 209-217.	5.8	231
5	Metal-free photoinduced electron transfer–atom transfer radical polymerization (PET–ATRP) via a visible light organic photocatalyst. Polymer Chemistry, 2016, 7, 689-700.	3.9	217
6	Albumin-NIR dye self-assembled nanoparticles for photoacoustic pH imaging and pH-responsive photothermal therapy effective for large tumors. Biomaterials, 2016, 98, 23-30.	11.4	182
7	A rice calcium-dependent protein kinase OsCPK9 positively regulates drought stress tolerance and spikelet fertility. BMC Plant Biology, 2014, 14, 133.	3.6	181
8	Hydrogen sulfide regulates abiotic stress tolerance and biotic stress resistance in <i>Arabidopsis</i> . Journal of Integrative Plant Biology, 2015, 57, 628-640.	8.5	161
9	<i>Dt2</i> ls a Gain-of-Function MADS-Domain Factor Gene That Specifies Semideterminacy in Soybean Â. Plant Cell, 2014, 26, 2831-2842.	6.6	136
10	Comprehensive characterization of distinct states of human naive pluripotency generated by reprogramming. Nature Methods, 2017, 14, 1055-1062.	19.0	128
11	Autophagy in sepsis: Degradation into exhaustion?. Autophagy, 2016, 12, 1073-1082.	9.1	111
12	Microbial degradation mechanism of pyridine by Paracoccus sp. NJUST30 newly isolated from aerobic granules. Chemical Engineering Journal, 2018, 344, 86-94.	12.7	86
13	The involvement of regulatory non-coding RNAs in sepsis: a systematic review. Critical Care, 2016, 20, 383.	5.8	79
14	Metalâ€Free Atom Transfer Radical Polymerization of Methyl Methacrylate with ppm Level of Organic Photocatalyst. Macromolecular Rapid Communications, 2017, 38, 1600461.	3.9	78
15	Aerobic granulation accelerated by biochar for the treatment of refractory wastewater. Chemical Engineering Journal, 2017, 314, 88-97.	12.7	77
16	Development of an indirect ELISA, blocking ELISA, fluorescent microsphere immunoassay and fluorescent focus neutralization assay for serologic evaluation of exposure to North American strains of Porcine Epidemic Diarrhea Virus. BMC Veterinary Research, 2015, 11, 180.	1.9	73
17	Photosensitizer cross-linked nano-micelle platform for multimodal imaging guided synergistic photothermal/photodynamic therapy. Nanoscale, 2016, 8, 15323-15339.	5.6	70
18	Aerobic granulation strategy for bioaugmentation of a sequencing batch reactor (SBR) treating high strength pyridine wastewater. Journal of Hazardous Materials, 2015, 295, 153-160.	12.4	64

#	Article	IF	CITATIONS
19	Conversion of waste FGD gypsum into hydroxyapatite for removal of Pb2+ and Cd2+ from wastewater. Journal of Colloid and Interface Science, 2014, 429, 68-76.	9.4	61
20	Enhanced pyridine biodegradation under anoxic condition: The key role of nitrate as the electron acceptor. Chemical Engineering Journal, 2015, 277, 140-149.	12.7	61
21	Characterization and Comparison of the Structural Features, Immune-Modulatory and Anti-Avian Influenza Virus Activities Conferred by Three Algal Sulfated Polysaccharides. Marine Drugs, 2016, 14, 4.	4.6	60
22	Neuroprotection by eIF2α-CHOP inhibition and XBP-1 activation in EAE/optic neuritiss. Cell Death and Disease, 2017, 8, e2936-e2936.	6.3	55
23	Atmospheric connections with the North Atlantic enhanced the deglacial warming in northeast China. Geology, 2017, 45, 1031-1034.	4.4	55
24	Self-assembly of BODIPY based pH-sensitive near-infrared polymeric micelles for drug controlled delivery and fluorescence imaging applications. Nanoscale, 2015, 7, 16399-16416.	5.6	54
25	Impact of Mongolian Plateau versus Tibetan Plateau on the westerly jet over North Pacific Ocean. Climate Dynamics, 2015, 44, 3067-3076.	3.8	50
26	Sleep Regulates Incubation of Cocaine Craving. Journal of Neuroscience, 2015, 35, 13300-13310.	3.6	49
27	Wogonin inhibits the proliferation and invasion, and induces the apoptosis of HepC2 and Bel7402 HCC cells through NF-κB/Bcl-2, ECFR and ECFR downstream ERK/AKT signaling. International Journal of Molecular Medicine, 2016, 38, 1250-1256.	4.0	48
28	Visible-light-induced living radical polymerization using in situ bromine-iodine transformation as an internal boost. Polymer Chemistry, 2017, 8, 2538-2551.	3.9	46
29	Catalyst-free iodine-mediated living radical polymerization under irradiation over a wide visible-light spectral scope. Polymer Chemistry, 2016, 7, 3576-3588.	3.9	44
30	Bioaugmentation potential of a newly isolated strain Sphingomonas sp. NJUST37 for the treatment of wastewater containing highly toxic and recalcitrant tricyclazole. Bioresource Technology, 2018, 264, 98-105.	9.6	44
31	Lactoferrin Inhibits IL-1β-Induced Chondrocyte Apoptosis Through AKT1-Induced CREB1 Activation. Cellular Physiology and Biochemistry, 2015, 36, 2456-2465.	1.6	43
32	Antibacterial and Cytotoxic Actinomycins Y ₆ –Y ₉ and Zp from <i>Streptomyces</i> sp. Strain Gö-GS12. Journal of Natural Products, 2016, 79, 2731-2739.	3.0	39
33	Exogenous application of ABA mimic 1 (AM1) improves cold stress tolerance in bermudagrass (Cynodon) Tj ETQq	1 <u>1 0</u> .784 2.3	•314 rgBT /O
34	Prolyl Hydroxylase Inhibitors Protect from the Bone Loss in Ovariectomy Rats by Increasing Bone Vascularity. Cell Biochemistry and Biophysics, 2014, 69, 141-149.	1.8	36
35	A direct discontinuous Galerkin method for the compressible Navier–Stokes equations on arbitrary grids. Journal of Computational Physics, 2016, 327, 484-502.	3.8	36
36	Bioaugmentation strategy for the treatment of fungicide wastewater by two triazole-degrading strains. Chemical Engineering Journal, 2018, 349, 17-24.	12.7	36

#	Article	IF	CITATIONS
37	Effect of Yunnan–Guizhou Topography at the Southeastern Tibetan Plateau on the Indian Monsoon. Journal of Climate, 2017, 30, 1259-1272.	3.2	35
38	Inhibition of AMPK/Autophagy Potentiates Parthenolideâ€Induced Apoptosis in Human Breast Cancer Cells. Journal of Cellular Biochemistry, 2014, 115, 1458-1466.	2.6	34
39	Magnetic nanomaterials with near-infrared pH-activatable fluorescence via iron-catalyzed AGET ATRP for tumor acidic microenvironment imaging. Journal of Materials Chemistry B, 2015, 3, 2786-2800.	5.8	33
40	Straightforward catalyst/solvent-free iodine-mediated living radical polymerization of functional monomers driven by visible light irradiation. Chemical Communications, 2016, 52, 10850-10853.	4.1	33
41	Removal of phosphate from etching wastewater by calcined alkaline residue: Batch and column studies. Journal of the Taiwan Institute of Chemical Engineers, 2014, 45, 1709-1716.	5.3	31
42	The Biosynthesis of Capuramycin-type Antibiotics. Journal of Biological Chemistry, 2015, 290, 13710-13724.	3.4	28
43	Water-use efficiency of an old-growth forest in lower subtropical China. Scientific Reports, 2017, 7, 42761.	3.3	28
44	Simultaneous pyridine biodegradation and nitrogen removal in an aerobic granular system. Journal of Environmental Sciences, 2018, 67, 318-329.	6.1	28
45	Up-regulation of Cathepsin G in the Development of Chronic Postsurgical Pain. Anesthesiology, 2015, 123, 838-850.	2.5	26
46	The enhanced atorvastatin hepatotoxicity in diabetic rats was partly attributed to the upregulated hepatic Cyp3a and SLCO1B1. Scientific Reports, 2016, 6, 33072.	3.3	26
47	Elevated Adenylyl Cyclase 9 Expression Is a Potential Prognostic Biomarker for Patients with Colon Cancer. Medical Science Monitor, 2018, 24, 19-25.	1.1	26
48	Optimizing production of hydroxyapatite from alkaline residue for removal of Pb2+ from wastewater. Applied Surface Science, 2014, 317, 946-954.	6.1	25
49	Acute liver failure impairs function and expression of breast cancerâ€resistant protein (<scp>BCRP</scp>) at rat blood–brain barrier partly via ammoniaâ€ <scp>ROS</scp> â€ <scp>ERK</scp> 1/2 activation. Journal of Neurochemistry, 2016, 138, 282-294.	3.9	25
50	Bioaugmentation of a continuous-flow self-forming dynamic membrane bioreactor for the treatment of wastewater containing high-strength pyridine. Environmental Science and Pollution Research, 2017, 24, 3437-3447.	5.3	25
51	Development of monoclonal antibodies and serological assays including indirect ELISA and fluorescent microsphere immunoassays for diagnosis of porcine deltacoronavirus. BMC Veterinary Research, 2016, 12, 95.	1.9	24
52	Donut shape plasma jet plumes generated by microwave pulses even without air mole fractions. Journal of Applied Physics, 2017, 121, .	2.5	23
53	Potential and use of bacterial small RNAs to combat drug resistance: a systematic review. Infection and Drug Resistance, 2017, Volume 10, 521-532.	2.7	22
54	Pathological Role and Diagnostic Value of Endogenous Host Defense Peptides in Adult and Neonatal Sepsis. Shock, 2017, 47, 673-679.	2.1	20

#	Article	IF	CITATIONS
55	A sustainable photocontrolled ATRP strategy: facile separation and recycling of a visible-light-mediated catalyst <i>fac</i> -[Ir(ppy) ₃]. Polymer Chemistry, 2018, 9, 584-592.	3.9	20
56	Transcription factorâ€mediated reprogramming: epigenetics and therapeutic potential. Immunology and Cell Biology, 2015, 93, 284-289.	2.3	18
57	New Monoclonal Antibodies to Defined Cell Surface Proteins on Human Pluripotent Stem Cells. Stem Cells, 2017, 35, 626-640.	3.2	18
58	Cholinergic tone in ventral tegmental area: Functional organization and behavioral implications. Neurochemistry International, 2018, 114, 127-133.	3.8	18
59	Synergistic effect of resveratrol and HSV-TK/GCV therapy on murine hepatoma cells. Cancer Biology and Therapy, 2019, 20, 183-191.	3.4	18
60	Decreased exposure of atorvastatin in diabetic rats partly due to induction of hepatic Cyp3a and Oatp2. Xenobiotica, 2016, 46, 875-881.	1.1	17
61	A biocatalytic approach to capuramycin analogues by exploiting a substrate permissive N-transacylase CapW. Organic and Biomolecular Chemistry, 2016, 14, 3956-3962.	2.8	16
62	Ataxiaâ€ŧelangiectasia mutated (<scp>ATM</scp>) participates in the regulation of ionizing radiationâ€induced cell death <i>via</i> MAPK14 in lung cancer H1299 cells. Cell Proliferation, 2015, 48, 561-572.	5.3	15
63	Hydrolysis and volatile fatty acids accumulation of waste activated sludge enhanced by the combined use of nitrite and alkaline pH. Environmental Science and Pollution Research, 2015, 22, 18793-18800.	5.3	15
64	Proprioceptive mechanisms in occlusionâ€stimulated masseter hypercontraction. European Journal of Oral Sciences, 2017, 125, 127-134.	1.5	15
65	5-nm LiF as an Efficient Cathode Buffer Layer in Polymer Solar Cells Through Simply Introducing a C60 Interlayer. Nanoscale Research Letters, 2017, 12, 543.	5.7	15
66	Acupuncture Treatment Reverses Retinal Gene Expression Induced by Optic Nerve Injury via RNA Sequencing Analysis. Frontiers in Integrative Neuroscience, 2019, 13, 59.	2.1	15
67	Effect of Acupuncture on Neuroplasticity of Stroke Patients with Motor Dysfunction: A Meta-Analysis of fMRI Studies. Neural Plasticity, 2021, 2021, 1-10.	2.2	15
68	Epigenetic memory in somatic cell nuclear transfer and induced pluripotency: Evidence and implications. Differentiation, 2014, 88, 29-32.	1.9	14
69	Dietary change in seabirds on Guangjin Island, South China Sea, over the past 1200 years inferred from stable isotope analysis. Holocene, 2017, 27, 331-338.	1.7	14
70	Spatial heterogeneity in stand characteristics alters water use patterns of mountain forests. Agricultural and Forest Meteorology, 2017, 236, 78-86.	4.8	13
71	The key role of biogenic manganese oxides in enhanced removal of highly recalcitrant 1,2,4-triazole from bio-treated chemical industrial wastewater. Environmental Science and Pollution Research, 2017, 24, 10570-10583.	5.3	12
72	GM-CSF and MEF-conditioned media support feeder-free reprogramming of mouse granulocytes to iPS cells. Differentiation, 2014, 87, 193-199.	1.9	11

#	Article	IF	CITATIONS
73	Preparation, characterization and adsorption properties of sodalite pellets. Materials Letters, 2014, 132, 259-262.	2.6	11
74	Evidence that oxidative dephosphorylation by the nonheme Fe(<scp>II</scp>), αâ€ketoglutarate: <scp>UMP</scp> oxygenase occurs by stereospecific hydroxylation. FEBS Letters, 2017, 591, 468-478.	2.8	11
75	Using Targeted Resequencing for Identification of Candidate Genes and SNPs for a QTL Affecting the pH Value of Chicken Meat. G3: Genes, Genomes, Genetics, 2015, 5, 2085-2089.	1.8	10
76	Changes in the source of sedimentary organic matter in the marginal sea sediments of Eastern Hainan Island in response to human activities during the past 200 years. Quaternary International, 2017, 440, 150-159.	1.5	10
77	Conserved termini and adjacent variable region of Twortlikevirus Staphylococcus phages. Virologica Sinica, 2015, 30, 433-440.	3.0	9
78	The Role of Deoxycytidine Kinase (dCK) in Radiation-Induced Cell Death. International Journal of Molecular Sciences, 2016, 17, 1939.	4.1	9
79	In vitro metabolism of l-corydalmine, a potent analgesic drug, in human, cynomolgus monkey, beagle dog, rat and mouse liver microsomes. Journal of Pharmaceutical and Biomedical Analysis, 2016, 128, 98-105.	2.8	9
80	Sensitive determination of glucose in Dulbecco's modified Eagle medium by highâ€performance liquid chromatography with 1â€phenylâ€3â€methylâ€5â€pyrazolone derivatization: application to gluconeogenesis studies. Biomedical Chromatography, 2016, 30, 601-605.	1.7	9
81	<i>Clostridium difficile</i> toxin B induces autophagic cell death in colonocytes. Journal of Cellular and Molecular Medicine, 2018, 22, 2469-2477.	3.6	9
82	Improvement of femoral component size prediction using a C-arm intensifier guide and our established algorithm in unicompartmental knee arthroplasty: A report from a Chinese population. Knee, 2014, 21, 435-438.	1.6	8
83	Interspecies differences in metabolism of deoxypodophyllotoxin in hepatic microsomes from human, monkey, rat, mouse and dog. Drug Metabolism and Pharmacokinetics, 2016, 31, 314-322.	2.2	8
84	Novel human H7N9 influenza virus in China. Integrative Zoology, 2014, 9, 372-375.	2.6	7
85	Paroxetine decreased plasma exposure of glyburide partly via inhibiting intestinal absorption in rats. Drug Metabolism and Pharmacokinetics, 2015, 30, 240-246.	2.2	7
86	Hydrolysis and acidification of waste activated sludge enhanced by zero valent iron-acid pretreatment: effect of pH. Desalination and Water Treatment, 2016, 57, 12099-12107.	1.0	7
87	Citrus Naringenin Increases Neuron Survival in Optic Nerve Crush Injury Model by Inhibiting JNK-JUN Pathway. International Journal of Molecular Sciences, 2022, 23, 385.	4.1	7
88	Correlation between δ ¹³ C and δ ¹⁵ N in flying fish (<i>Exocoetus volitans</i>) muscle and scales from the South China Sea. Oceanological and Hydrobiological Studies, 2017, 46, 307-313.	0.7	6
89	Mineral magnetic record of the Miocene-Pliocene climate transition on the Chinese Loess Plateau, North China. Quaternary Research, 2018, 89, 619-628.	1.7	6
90	Effects of Retinal Transcription Regulation After GB20 Needling Treatment in Retina With Optic Neuritis. Frontiers in Integrative Neuroscience, 2020, 14, 568449.	2.1	6

#	Article	IF	CITATIONS
91	Complete Genome Sequence of Multidrug-Resistant Citrobacter freundii Strain P10159, Isolated from Urine Samples from a Patient with Esophageal Carcinoma. Genome Announcements, 2016, 4, .	0.8	5
92	Co-administration of paroxetine increased the systemic exposure of pravastatin in diabetic rats due to the decrease in liver distribution. Xenobiotica, 2015, 45, 794-802.	1.1	3
93	Recycling Phosphated Residue for Pb ²⁺ Removal from Wastewater. Environmental Engineering Science, 2016, 33, 207-214.	1.6	3
94	Simultaneous Determination of Deoxypodophyllotoxin and Its Major Metabolites in Rat Plasma by a Sensitive LC–MS/MS Method and Its Application in a Pharmacokinetic Study. Chromatographia, 2016, 79, 53-61.	1.3	2
95	Performance evaluation and kinetics study of Paracoccus versutus and Shinella granuli newly isolated from pyridine-degrading aerobic granules. , 0, 81, 162-169.		2